Service

Spotlight on Angewandte's Sister Journals 9476 – 9479

Author Profile

Jianbo Wang 9482

"When I was eighteen I wanted to be an agriculturist. If I could be described as an animal it would be a panda …"
This and more about Jianbo Wang can be found on page 9482.

Obituaries

William Standish Knowles (1917–2012)

D. Ager, A. Chan, S. Laneman, J. Talley* **9483 – 9484**

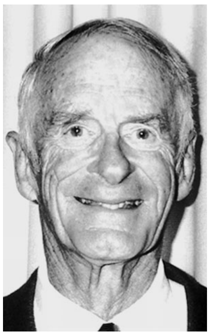

William S. Knowles, who received the 2001 Nobel Prize in Chemistry for his work on asymmetric catalysis, and particular hydrogenation reactions, passed away in June 2012.

Books

Introduction to Membrane Science and Technology Heinrich Strathmann *reviewed by B. Freeman* **9485**

Highlights

Asymmetric Catalysis

M. Wilsdorf, H.-U. Reissig* **9486 – 9488**

Simple, but Challenging: Recent Developments in the Asymmetric Synthesis of Spiroketals

Impressive and elegant approaches to the enantioselective synthesis of spiroketals starting from achiral substrates have been described recently. These strategies based on transition-metal catalysis and organocatalysis hold great potential for further applications.

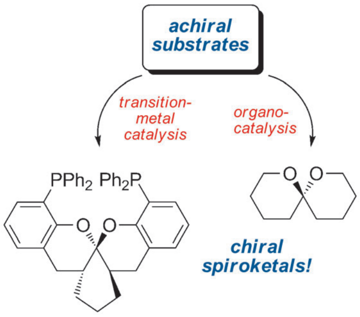

Coupled Oscillators

M. Bär,* E. Schöll, A. Torcini **9489 – 9490**

Synchronization and Complex Dynamics of Oscillators with Delayed Pulse Coupling

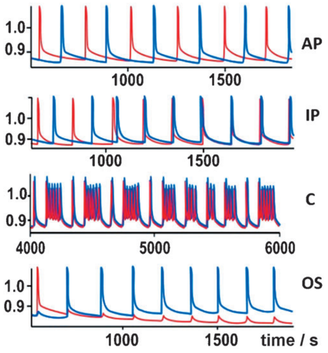

Finger on the pulse: A systematic experimental study of pulse-coupled chemical oscillators with delay has confirmed a surprisingly large number of theoretical and mathematical predictions (see the dynamics for a pair of pulse-coupled oscillators; AP = antiphase (AP) and IP = in-phase oscillations, C = complex bursting dynamics, and OS = oscillator suppression). These results have implications for neuroscience and other biological fields.

Reviews

Polyoxometalates

N. V. Izarova,* M. T. Pope,* U. Kortz* ______________ **9492 – 9510**

Noble Metals in Polyoxometalates

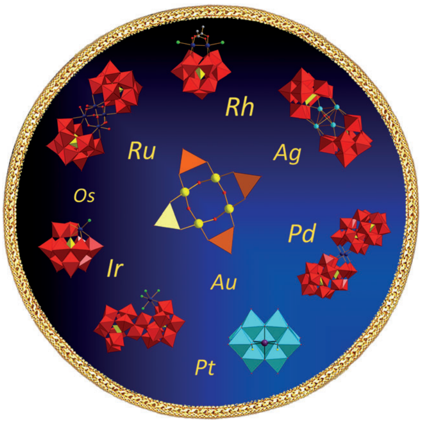

Polyoxometalates strike it rich: Discrete polyoxometalates containing noble metals (ruthenium, osmium, rhodium, palladium, platinum, silver, and gold, see picture) form a rich class of compounds. It includes both classical heteropolyanions (vanadates, molybdates, tungstates) where noble metals are present as heteroatoms, as well as the recently discovered novel subclass of polyoxometalates constructed of noble-metal addenda atoms.

Communications

Asymmetric Catalysis

M. Potowski, J. O. Bauer, C. Strohmann, A. P. Antonchick,* H. Waldmann* ______________ **9512 – 9516**

Highly Enantioselective Catalytic [6+3] Cycloadditions of Azomethine Ylides

Frontispiece

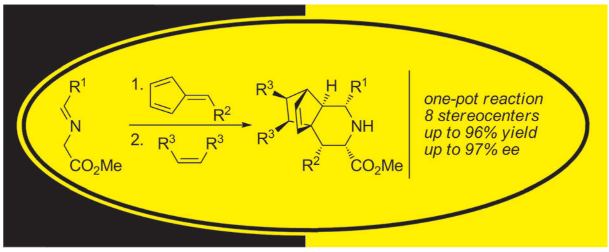

Under control: Highly functionalized chiral annulated piperidines with eight stereocenters are efficiently obtained by means of a highly enantioselective one-pot [6+3]/[4+2] sequence. This sequence included the first enantioselective [6+3] cycloaddition of azomethine ylides with fulvenes.

For the USA and Canada:
ANGEWANDTE CHEMIE International Edition (ISSN 1433-7851) is published weekly by Wiley-VCH, PO Box 191161, 69451 Weinheim, Germany. Air freight and mailing in the USA by Publications Expediting Inc., 200 Meacham Ave., Elmont, NY 11003. Periodicals postage paid at Jamaica, NY 11431. US POSTMASTER: send address changes to *Angewandte Chemie*, Journal Customer Services, John Wiley & Sons Inc., 350 Main St., Malden, MA 02148-5020. Annual subscription price for institutions: US$ 11.738/10.206 (valid for print and electronic / print or electronic delivery); for individuals who are personal members of a national chemical society prices are available on request. Postage and handling charges included. All prices are subject to local VAT/ sales tax.

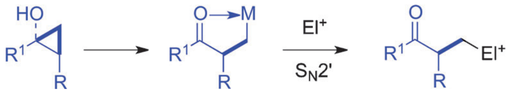

Reining in reactivity: Stereoselective $\mathrm{S_N}2'$ alkylation of cyclopropanols has been devised under the control of mixed zinc/copper reagents. This method provides convenient access to enantiopure keto homoenolates which react with electrophiles (El$^+$) to form C–C bonds. M = metal.

Synthetic Methods

P. P. Das, K. Belmore,
J. K. Cha* **9517–9520**

$\mathrm{S_N}2'$ Alkylation of Cyclopropanols via Homoenolates

---

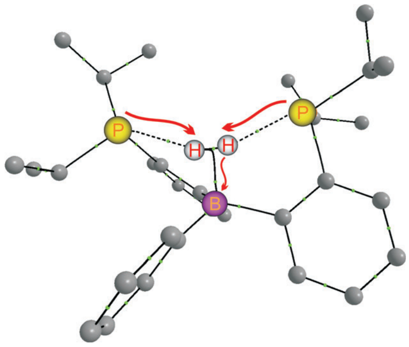

A bit on the side: A computational study of the reaction between a diphosphinoborane and dihydrogen has shown that, in marked contrast to other FLP systems, the reaction involves a symmetric dihydrogen complex as an intermediate. Thorough analysis has revealed an unusual bonding situation, namely side-on coordination of H_2 to the central boron center and weak contacts with the peripheral donor phosphine groups (see calculated structure).

Dihydrogen Complexes

L. Könczöl, E. Makkos, D. Bourissou,*
D. Szieberth* **9521–9524**

Computational Evidence for a New Type of η^2-H_2 Complex: When Main-Group Elements Act in Concert To Emulate Transition Metals

---

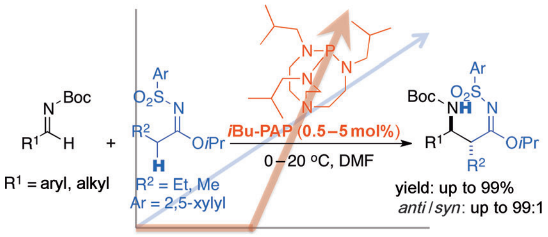

First walk, then run! Highly efficient organosuperbase-catalyzed Mannich-type reactions of sulfonylimidates with readily prepared Boc-protected imines have been developed. The desired products were obtained in high yield and with high *anti* selectivity. Mechanistic studies show an induction period for the catalyzed reaction, and that the organosuperbase works as an initiator.

Organocatalysis

J. Nakano, K. Masuda, Y. Yamashita,
S. Kobayashi* **9525–9529**

Highly Efficient Organosuperbase-Catalyzed Mannich-type Reactions of Sulfonylimidates with Imines: Successful Use of Aliphatic Imines as Substrates and a Unique Reaction Mechanism

---

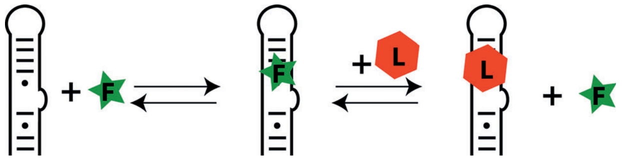

Spy swap: The interaction between an unlabeled RNA and unlabeled ligands (red hexagon) can be monitored by ^{19}F NMR spectroscopy using small fluorinated diamines (green star) as spy reporters (see scheme). This technique also enables the visualization of the conformational capture of a riboswitch by its ligand.

RNA Structures

T. Lombès, R. Moumné, V. Larue, E. Prost,
M. Catala, T. Lecourt, F. Dardel,
L. Micouin,* C. Tisné* **9530–9534**

Investigation of RNA–Ligand Interactions by ^{19}F NMR Spectroscopy Using Fluorinated Probes

The German Chemical Society (GDCh) invites you to:

Angewandte 125 JAHRE Anniversary Symposium

Eine Zeitschrift der Gesellschaft Deutscher Chemiker

GDCh

Tuesday, March 12, 2013

Henry Ford Building / FU Berlin

Speakers


Carolyn R. Bertozzi


François Diederich


Alois Fürstner


Roald Hoffmann
(Nobel Prize 1981)


Susumu Kitagawa


Jean-Marie Lehn
(Nobel Prize 1987)


E.W. “Bert” Meijer


Frank Schirrmacher
(Publisher, *FAZ*)


Robert Schlögl


George M. Whitesides


Ahmed Zewail
(Nobel Prize 1999)

More information:

Freie Universität Berlin

angewandte.org/symposium

WILEY-VCH

GDCh
GESELLSCHAFT
DEUTSCHER CHEMIKER

C–F Bond Activation

T. Iida, R. Hashimoto, K. Aikawa, S. Ito,
K. Mikami* ________ **9535 – 9538**

Umpolung of Fluoroform by C–F Bond Activation: Direct Difluoromethylation of Lithium Enolates

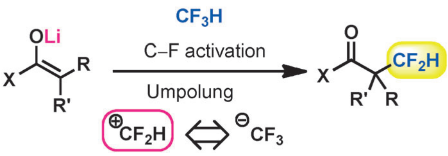

Double agent: The direct α-difluoromethylation of lithium enolates using an umpolung form of fluoroform as a difluoromethyl carbocation equivalent leads to an all-carbon quaternary center. Late transition metals are not necessary and the reaction involves activation of inert C–F bonds with subsequent C–C bond formation.

Asymmetric Autocatalysis

T. Gehring, M. Quaranta, B. Odell,
D. G. Blackmond,*
J. M. Brown* ________ **9539 – 9542**

Observation of a Transient Intermediate in Soai's Asymmetric Autocatalysis: Insights from ^{1}H NMR Turnover in Real Time

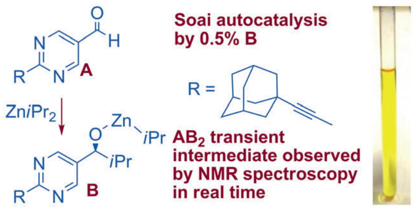

Caught in the act: ^{1}H NMR spectroscopy was used to monitor the loss of reactant and formation of product during the induction and burst phases of Soai's autocatalysis reaction. A transient intermediate was observed at 0 °C and identified as an alkoxyacetal formed from one aldehyde and two alkoxide moieties (see picture).

Heterogeneous Catalysis

VIP

K. Yoon, Y. Yang, P. Lu, D. Wan, H. Peng,
K. Stamm Masias, P. T. Fanson,
C. T. Campbell, Y. Xia* ________ **9543 – 9546**

A Highly Reactive and Sinter-Resistant Catalytic System Based on Platinum Nanoparticles Embedded in the Inner Surfaces of CeO$_2$ Hollow Fibers

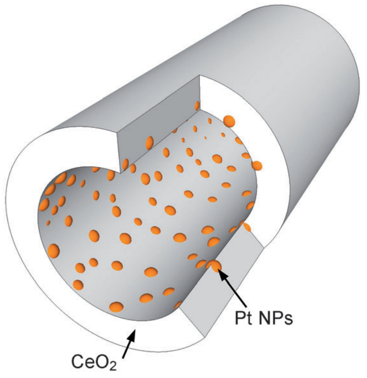

Ceria (CeO$_2$) hollow fibers with Pt nanoparticles (Pt NPs) embedded in their inner surfaces were prepared by sequentially depositing Pt NPs and CeO$_2$ sheaths on electrospun fibers of polystyrene, followed by calcination in air at 400 °C. Despite a relatively low Pt loading in this system, the turnover frequency for CO oxidation was 2–3 orders of magnitude higher than those of other systems, and the reactivity was also stable up to 700 °C.

Cross-Coupling Reactions

Y. Weng, B. Cheng, C. He,
A. Lei* ________ **9547 – 9551**

Rational Design of a Palladium-Catalyzed C$_{sp}$–C$_{sp}$ Cross-Coupling Reaction Inspired by Kinetic Studies

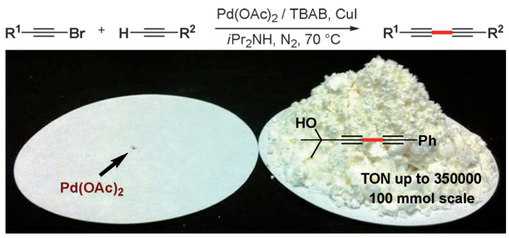

Less is More: A highly selective Pd-catalyzed C$_{sp}$–C$_{sp}$ cross-coupling reaction between terminal alkynes and 1-bromoacetylenes has been developed. Catalyst loading is low (only 0.0001–0.01 mol % of Pd is required) and provides products with high selectivities and good to excellent yields under mild conditions. TBAB = tetrabutylammonium bromide, TON = turnover number.

Protein Structures

A. Giuliani,* A. R. Milosavljević,
K. Hinsen, F. Canon, C. Nicolas,
M. Réfrégiers, L. Nahon ____ 9552–9556

Structure and Charge-State Dependence of the Gas-Phase Ionization Energy of Proteins

Photoionization of protein ions: The ionization energy of polyprotonated protein cations in the gas phase measured using VUV synchrotron radiation appears to be correlated with the charge state *z* of the protein and its tertiary structure. A simple electrostatic model accounts for the results and also shows predictive capabilities to derive a mean radius R_m of the protein ion from the ionization energy, and vice versa.

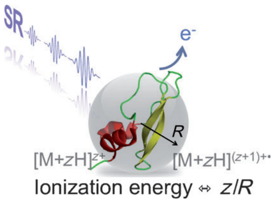

Low-Coordinate Cations

J. Li, C. Schenk, F. Winter, H. Scherer,
N. Trapp, A. Higelin, S. Keller, R. Pöttgen,
I. Krossing,* C. Jones* ____ 9557–9561

Weak Arene Stabilization of Bulky Amido-Germanium(II) and Tin(II) Monocations

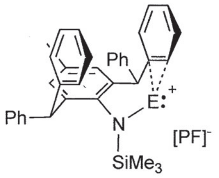

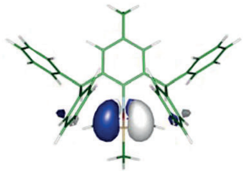

Guilty as charged: Germanium(II) and tin(II) monocations which are stabilized by an extremely bulky amido ligand and a very weakly coordinating anion are reported (see picture; E = Ge, Sn; PF = $[Al\{OC(CF_3)_3\}_4]^-$). The metal centers exhibit weak intramolecular η^2-arene interactions, and preliminary reactivity studies highlight the electrophilicity of the cations.

Photocatalysis

S. Maity, N. Zheng* ______ 9562–9566

A Visible-Light-Mediated Oxidative C–N Bond Formation/Aromatization Cascade: Photocatalytic Preparation of *N*-Arylindoles

Just add light and air: Structurally diverse *N*-arylindoles can be prepared from readily prepared *o*-styryl anilines through visible-light photocatalysis. The reaction, which is conducted open to air, is mediated by $[Ru(bpz)_3](PF_6)_2$ (bpz = 2,2′-bipyrazine) and involves both C–N bond formation and aromatization (see scheme). Using suitably substituted substrates, a 1,2-carbon shift can be also incorporated into this cascade reaction.

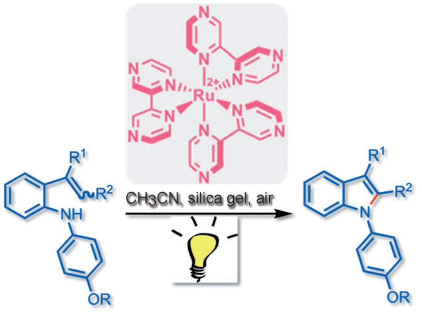

Synthetic Methods

Y. Yasu, T. Koike,* M. Akita* 9567–9571

Three-component Oxytrifluoromethylation of Alkenes: Highly Efficient and Regioselective Difunctionalization of C=C Bonds Mediated by Photoredox Catalysts

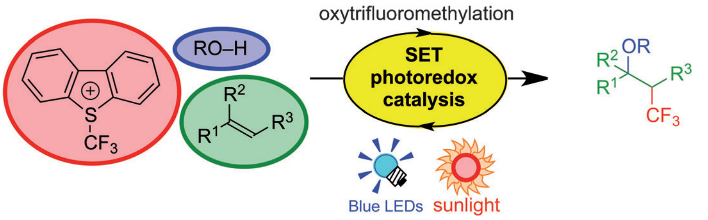

Here comes the sun: A facile vicinal difunctionalization of alkenes, oxytrifluoromethylation, was established by visible-light-driven photoredox catalysis. Judicious choice of the CF_3 source is key. Nucleophiles such as water, alcohols, and carboxylic acids can be used in this highly efficient (2–4 h) and regioselective (100 %) transformation using light-emitting diode (LED) lamps and natural sunlight. SET = single-electron transfer.

Gold Catalysis

S. G. Modha, A. Kumar, D. D. Vachhani, J. Jacobs, S. K. Sharma, V. S. Parmar, L. Van Meervelt, E. V. Van der Eycken* ______ 9572 – 9575

A Diversity-Oriented Approach to Spiroindolines: Post-Ugi Gold-Catalyzed Diastereoselective Domino Cyclization

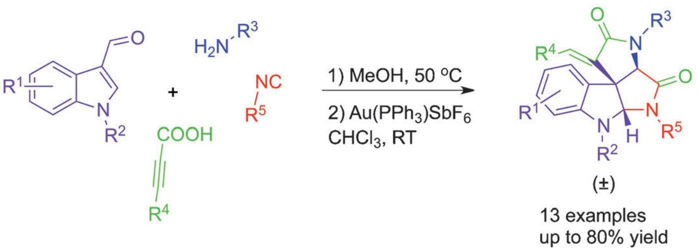

Caught "Spiro" handed: A diversity-oriented approach comprised of an Ugi four-component reaction and a diastereoselective gold(I)-catalyzed domino cyclization for the generation of complex spiroindolines under mild conditions has been developed. Variously substituted spiroindolines were synthesized in good to excellent yields and with complete diastereoselectivity.

Total Synthesis

M. J. Schnermann, L. E. Overman* ______ 9576 – 9580

A Concise Synthesis of (−)-Aplyviolene Facilitated by a Strategic Tertiary Radical Conjugate Addition

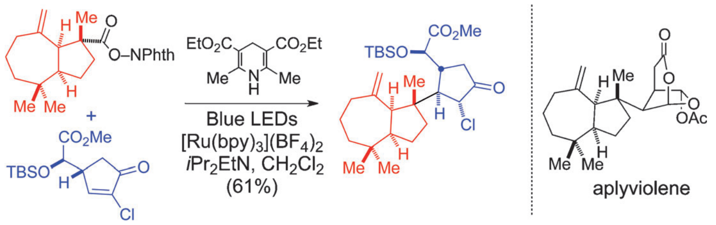

A second-generation synthesis of the rearranged spongian diterpene aplyviolene is reported. The key step is the addition of a trialkyl tertiary radical generated by photoredox-mediated fragmentation of a N-(acyloxy)phthalimide to an α-chloropentenone (see scheme). This process fashioned a quaternary stereocenter while combining two units of significant complexity.

Synthetic Methods

M. J. Schnermann, N. L. Untiedt, G. Jiménez-Osés, K. N. Houk,* L. E. Overman* ______ 9581 – 9586

Forming Tertiary Organolithiums and Organocuprates from Nitrile Precursors and their Bimolecular Reactions with Carbon Electrophiles to Form Quaternary Carbon Stereocenters

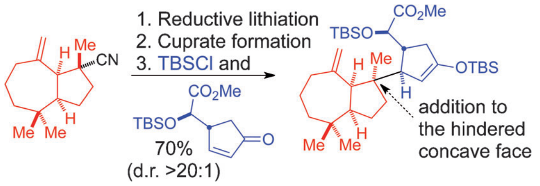

Unstabilized tertiary organolithium intermediates are conveniently generated by reductive decyanation of nitriles, and these reagents and their derived cuprates couple in useful yields with carbon-centered electrophiles (see example). Chiral tertiary organolithium and organocuprate derivatives of substituted *cis*-perhydroazulenes and *cis*-perhydropentalenes react with electrophiles with high diastereoselectivity from the more-hindered concave face.

Natural Product Synthesis

M. Henrot, M. E. A. Richter, J. Maddaluno, C. Hertweck,* M. De Paolis* ______ 9587 – 9591

Convergent Asymmetric Synthesis of (+)-Aureothin Employing an Oxygenase-Mediated Resolution Step

Front Cover

Need an enzymatic push? The desymmetrization of α,α′-dimethoxy-γ-pyrone allows the convergent and rapid preparation of the complete carbon skeleton of (+)-aureothin (see scheme). The final step in the synthesis of the target molecule is the regiodivergent parallel kinetic resolution promoted by cytochrome P450 monooxygenase AurH to deliver the enantiopure natural product.

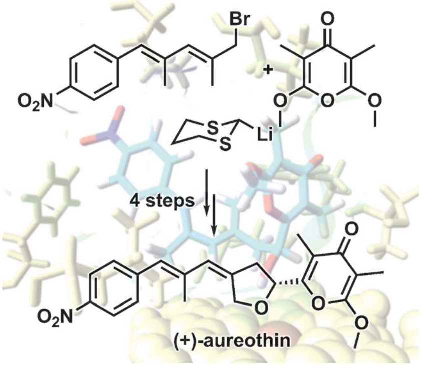

Cathode Materials

C. F. Zhang, H. B. Wu, C. Z. Yuan, Z. P. Guo,* X. W. Lou* ______ 9592 – 9595

Confining Sulfur in Double-Shelled Hollow Carbon Spheres for Lithium–Sulfur Batteries

Inside Cover

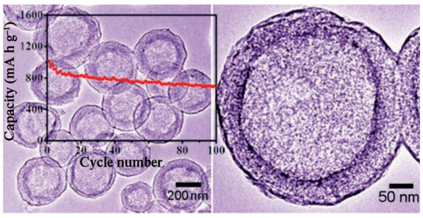

Going into their shell: A novel carbon–sulfur nanocomposite has been synthesized by confining sulfur in double-shelled "soft" carbon hollow spheres (see figure) with high surface area and porosity. This carbon–sulfur nanocomposite shows outstanding electrochemical performance when evaluated as a cathode material for lithium–sulfur batteries.

Sensors

A. Mathew, P. R. Sajanlal, T. Pradeep* ______ 9596 – 9600

Selective Visual Detection of TNT at the Sub-Zeptomole Level

Inside Back Cover

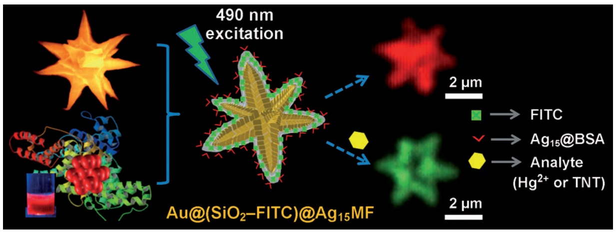

How low can you go? The visual detection of 2,4,6-trinitrotoluene and Hg^{2+} at the sub-zeptomole level is demonstrated. This was achieved using a hybrid material that allowed for the development of a single-particle, single-molecule detection technique, which may be the ultimate in ultra-trace sensitivity with selectivity.

Water Splitting

K. S. Joya,* N. K. Subbaiyan, F. D'Souza, H. J. M. de Groot* ______ 9601 – 9605

Surface-Immobilized Single-Site Iridium Complexes for Electrocatalytic Water Splitting

Back Cover

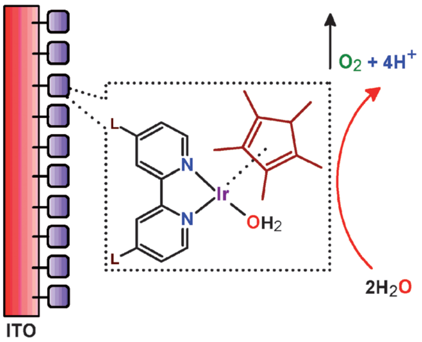

Water into oxygen: Mono-iridium complexes (see picture; L = PO_3H_2 or COOH) were immobilized on an indium tin oxide (ITO) surface to form a molecular electrocatalytic water oxidation assembly that mimics photosystem II in producing molecular oxygen with high turnover numbers (TONs). The catalyst shows TONs for O_2 higher than 210000 and turnover frequencies higher than 6.7 s^{-1} during electrochemical catalytic water splitting.

Biosensors

A. J. Boersma, H. Bayley* — **9606 – 9609**

Continuous Stochastic Detection of Amino Acid Enantiomers with a Protein Nanopore

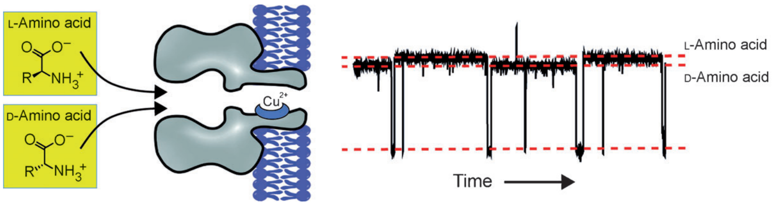

A stochastic sensing method: Discrimination between enantiomeric amino acids is achieved when the amino acids bind to a Cu^{II} complex within a protein nanopore sensor, which provides a chiral environment. The potential of the method is demonstrated by real-time observation of the increase in enantiomeric excess during an enzymatic kinetic resolution.

Homogeneous Catalysis

B.-H. Tan, J. Dong,
N. Yoshikai* ——— **9610 – 9614**

Cobalt-Catalyzed Addition of Arylzinc Reagents to Alkynes to Form *ortho*-Alkenylarylzinc Species through 1,4-Cobalt Migration

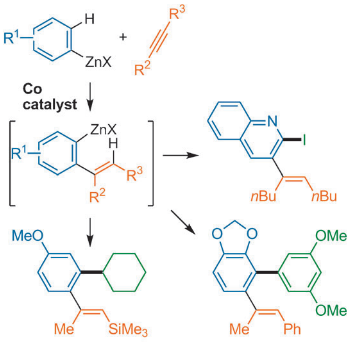

Migratory carbometalation: A cobalt–Xantphos complex catalyzes the addition of an arylzinc reagent to an unactivated internal alkyne; the reaction most likely involves insertion of the alkyne into an arylcobalt species and vinyl-to-aryl 1,4-cobalt migration, followed by transmetalation with the arylzinc reagent. Interception of the resulting *ortho*-alkenylarylzinc species with electrophiles allows access to 1-alkenyl arenes functionalized in the 2-position.

Natural Products

K. Scherlach, B. Busch, G. Lackner,
U. Paszkowski,
C. Hertweck* ——— **9615 – 9618**

Symbiotic Cooperation in the Biosynthesis of a Phytotoxin

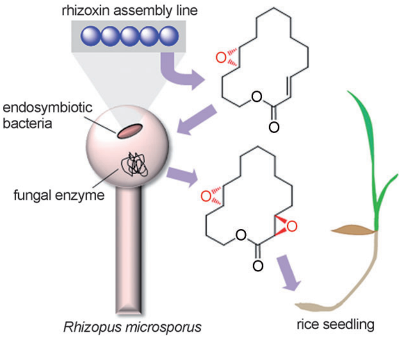

Division of labor: A combination of genetic, microbial, and chemical analyses solved the riddle of the dual epoxidation in the biosynthesis of rhizoxin, the causative agent of rice seedling blight. Bacterial endosymbionts of *Rhizopus microsporus* mediate the first epoxidation by a dedicated cytochrome P450 monooxygenase. The second oxirane ring is introduced by the fungal host and results in a substantially increased potency of the phytotoxin.

Micromachining

J.-H. Huang, A. Jayaraman,
V. M. Ugaz* ——— **9619 – 9623**

Enzymatic Sculpting of Nanoscale and Microscale Surface Topographies

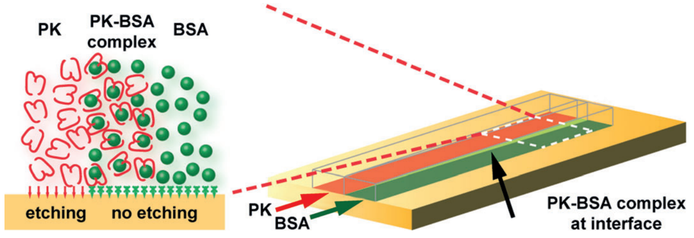

Lithography-free etching of complex surface features is achieved by harnessing the enzyme proteinase K (PK), controlled by bovine serum albumin (BSA), to digest a biodegradable polymer. This bio-sculpting process is used to construct a membraneless filtration device for the size-based isolation and enrichment of cells from whole blood.

Luminescence

L. K. Truman, S. Comby,*
T. Gunnlaugsson* ———— **9624 – 9627**

pH-Responsive Luminescent Lanthanide-Functionalized Gold Nanoparticles with "On–Off" Ytterbium Switchable Near-Infrared Emission

A pH indicator: Near-infrared emitting lanthanide-functionalized gold nanoparticles have been prepared through self-assembly at the gold surface between a ytterbium(III)–cyclen complex and xylenol orange (see picture). Excitation of the xylenol orange unit with visible light, up to 600 nm, results in the sensitization of the Yb^{III}-centered near-infrared emission that can be reversibly switched "on–off" as a function of the pH value.

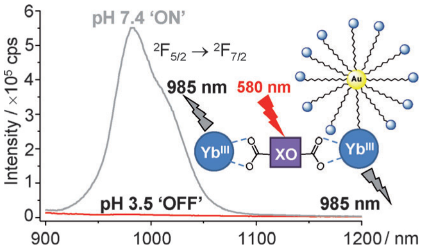

Catalytic Oxidation

C. Zhang, F. Liu, Y. Zhai, H. Ariga, N. Yi,
Y. Liu, K. Asakura,
M. Flytzani-Stephanopoulos,*
H. He* ———— **9628 – 9632**

Alkali-Metal-Promoted Pt/TiO_2 Opens a More Efficient Pathway to Formaldehyde Oxidation at Ambient Temperatures

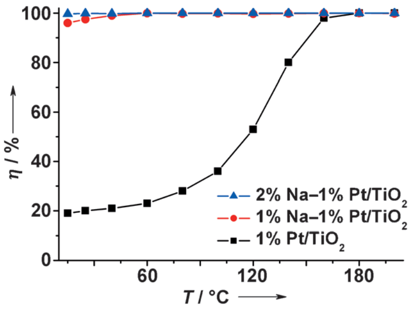

Addition of alkali metal ions significantly promotes the activity of the Pt/TiO_2 catalyst for the HCHO oxidation reaction by stabilizing an atomically dispersed $Pt-O(OH)_x$ alkali metal species and opening a new low-temperature reaction pathway. The atomically dispersed $Na-Pt-O(OH)_x$ species can effectively activate H_2O and catalyze the facile reaction between surface OH and formate species to total oxidation products.

Delivery Systems

D. Jiao, J. Geng, X. J. Loh, D. Das,
T.-C. Lee, O. A. Scherman* — **9633 – 9637**

Supramolecular Peptide Amphiphile Vesicles through Host–Guest Complexation

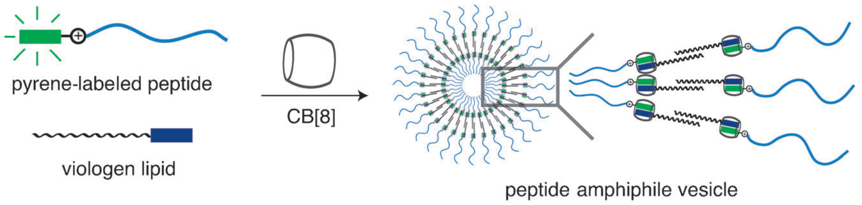

Tricky triggering: Supramolecular peptide amphiphiles were prepared by host–guest complexation of pyrene-labeled peptides and viologen lipid with cucurbit[8]uril. They self-assemble into vesicles, which are responsive to a variety of external triggers. Both "switching on" and "switching off" of fluoresence and cytotoxicity is demonstrated in vitro.

Asymmetric Organocatalysis

X. Yang, P. Liu, K. N. Houk,*
V. B. Birman* ———— **9638 – 9642**

Manifestation of Felkin–Anh Control in Enantioselective Acyl Transfer Catalysis: Kinetic Resolution of Carboxylic Acids

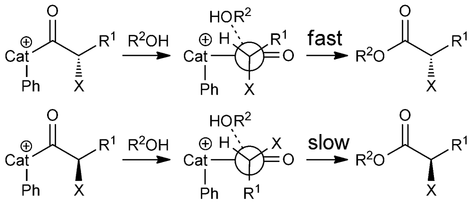

Under control: The classical polar Felkin–Anh model has been applied for the first time to the analysis of diastereoselectivity in acylation reactions (see scheme). Computational studies demonstrate that stereoelectronic effects control the enantioselectivity in asymmetric catalytic alcoholysis of acyclic anhydrides.

Sensors

K. Sakakibara, L. A. Joyce, T. Mori,
T. Fujisawa, S. H. Shabbir, J. P. Hill,
E. V. Anslyn,* K. Ariga* ____ **9643–9646**

A Mechanically Controlled Indicator Displacement Assay

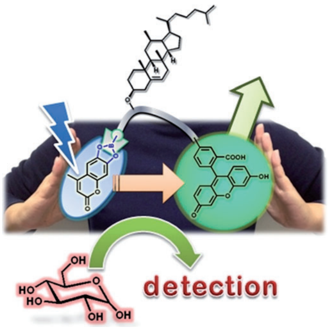

Push a host: Mechanical compression was applied to a host monolayer at an interface, which facilitated an indicator displacement assay. The fluorescence resonance energy transfer (FRET) between the host and indicator was switched on by this compression. Addition of D-glucose caused the indicator to be displaced, effectively quenching the FRET process.

Soft Matter

A. Stocco,* M. Chanana, G. Su,
P. Cernoch, B. P. Binks,
D. Wang* ____ **9647–9651**

Bidirectional Nanoparticle Crossing of Oil–Water Interfaces Induced by Different Stimuli: Insight into Phase Transfer

Swap transactions: Bidirectional spontaneous transfer of gold nanoparticles coated with stimuli-responsive polymer brushes across oil–water interfaces has been implemented (see picture). The water-to-oil transfer of the gold nanoparticles is dictated by the ionic strength in water, while the nanoparticle oil-to-water transfer occurs only when the environmental temperature is reduced below 5 °C.

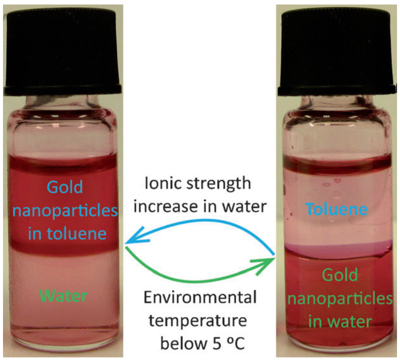

Biosensors

J. Wang, J. Karpus, B. Zhao, Z. Luo,
P. R. Chen, C. He* ____ **9652–9656**

A Selective Fluorescent Probe for Carbon Monoxide Imaging in Living Cells

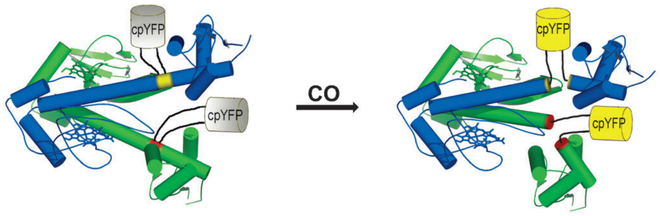

A genetically encoded fluorescent probe is capable of selectively detecting carbon monoxide inside living cell. The probe, named COSer (CO sensor), consists of a circularly permuted yellow fluorescent protein (cpYFP) inserted into the regulatory domain of the bacterial CO-sensing protein, CooA, which gives the probe its selective CO-binding property.

Intracellular pH Sensing

M. J. Marín, F. Galindo,* P. Thomas,
D. A. Russell* ____ **9657–9661**

Localized Intracellular pH Measurement Using a Ratiometric Photoinduced Electron-Transfer-Based Nanosensor

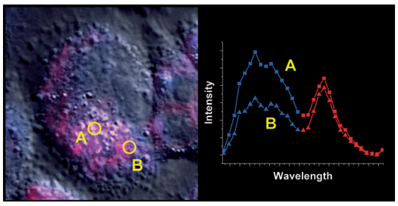

Intracellular analysis: Changes in the concentration of hydrogen ions can lead to cellular dysfunction. Thus, quantification of the intracellular pH in localized compartments (see A and B) is important. A pH nanosensor based on photoinduced electron transfer is described that targets acidic organelles. A combination of confocal fluorescence microscopy and spectroscopy is used for localized pH measurements within living cells.

Cluster Compounds

D. Cauzzi, R. Pattacini, M. Delferro,
F. Dini, C. Di Natale, R. Paolesse,
S. Bonacchi, M. Montalti, N. Zaccheroni,
M. Calvaresi, F. Zerbetto,
L. Prodi* ________ **9662 – 9665**

Temperature-Dependent Fluorescence of Cu_5 Metal Clusters: A Molecular Thermometer

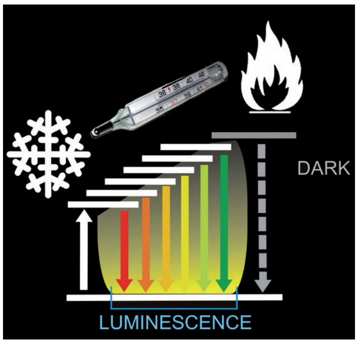

The heat is on: A Cu_5 metal cluster presents distinctive photophysical properties that result in a temperature-dependent fluorescent quantum yield and excited-state lifetime between -45 and $+80\,^{\circ}$C, both in solution and as a solid. Unprecedented accuracy in temperature determination by fluorescence measurements was achieved with this complex, thus making it suitable for applications in, for example, biology and (nano)materials research.

Protein Dynamics

P. Liuni, A. Jeganathan,
D. J. Wilson* ________ **9666 – 9669**

Conformer Selection and Intensified Dynamics During Catalytic Turnover in Chymotrypsin

Intensified searching: In enzymes, conformational dynamics are linked to the catalytic reaction coordinate. A novel analytical approach was used to monitor catalysis-linked dynamics in chymotrypsin, revealing that in some enzymes, catalysis is promoted by intensified, but undirected conformational sampling after substrate binding.

Nanobiomaterials

J. H. Kim, Y.-W. Noh, M. B. Heo,
M. Y. Cho, Y. T. Lim* ________ **9670 – 9673**

Multifunctional Hybrid Nanoconjugates for Efficient In Vivo Delivery of Immunomodulating Oligonucleotides and Enhanced Antitumor Immunity

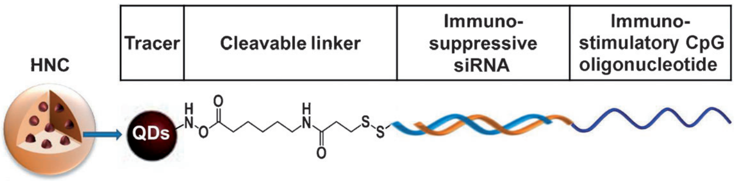

A winning combination: Multifunctional hybrid nanoconjugates (HNCs) based on polymer nanoparticles containing quantum dots (QDs) conjugated with CpG oligonucleotides (as a ligand for TLR9) and STAT3 siRNAs (to suppress the immune response) have been synthesized (see scheme). These HNCs were shown to synergistically enhance the antitumor immune response in dendritic cells and in tumor-bearing mice.

Natural Product Synthesis

A. Y. Hong, B. M. Stoltz* ___ **9674 – 9678**

Enantioselective Total Synthesis of the Reported Structures of (−)-9-*epi*-Presilphiperfolan-1-ol and (−)-Presilphiperfolan-1-ol: Structural Confirmation and Reassignment and Biosynthetic Insights

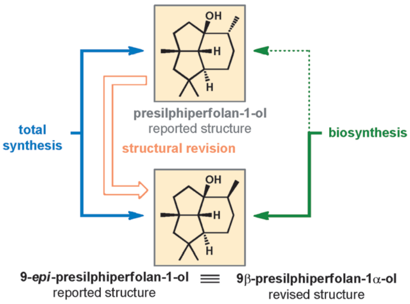

When *epi* isn't! The first total synthesis of the reported structures of 9-*epi*-presilphiperfolan-1-ol and presilphiperfolan-1-ol has been achieved. Key steps are a catalytic asymmetric alkylation of a novel diene-containing electrophile followed by a two-carbon ring contraction and an intramolecular Diels–Alder cycloaddition to form the stereochemically dense tricyclic core. The synthetic work has resulted in the structural revision of presilphiperfolan-1-ol (see scheme).

Photochemistry

S. Yagai,* K. Iwai, T. Karatsu,
A. Kitamura ______ **9679 – 9683**

Photoswitchable Exciton Coupling in Merocyanine–Diarylethene Multi-Chromophore Hydrogen-Bonded Complexes

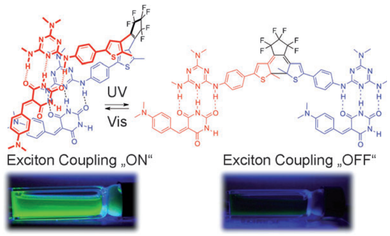

Light on: Photocontrol of J-type exciton interactions by using chromophores is reported (see picture). Hydrogen-bonded merocyanine dyes could be switched reversibly through photoinduced ring-closure/ring-opening reactions of diarylethene receptors. Addition of H-aggregation-inducing bismelamine receptors enabled the partial interconversion between J- and H-type exciton coupling.

Enantioselective Fluorination

T. Honjo, R. J. Phipps, V. Rauniyar,
F. D. Toste* ______ **9684 – 9688**

A Doubly Axially Chiral Phosphoric Acid Catalyst for the Asymmetric Tandem Oxyfluorination of Enamides

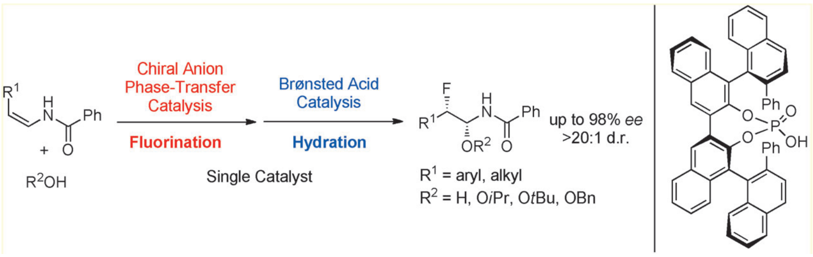

Double agent: Enantioselective tandem oxyfluorination of enamides using a doubly axially chiral phosphoric acid catalyst is reported. The chiral phosphoric acid catalyst controls both a fluorination step, using a chiral anion phase-transfer strategy, and addition to the resulting imine under the guise of Brønsted acid catalysis.

Nanomaterials

Dr. X.-H. Li,* S. Kurasch, U. Kaiser,
M. Antonietti* ______ **9689 – 9692**

Synthesis of Monolayer-Patched Graphene from Glucose

Graphene patchwork: A simple synthetic process requiring neither catalyst nor solvent was used to convert glucose directly into polycrystalline carbon sheets having a "patched" multidomain graphene structure with domains 2–15 nm in size. The carbon assemblies exhibit high conductivity, high specific surface area, and an unexpectedly good solution processability.

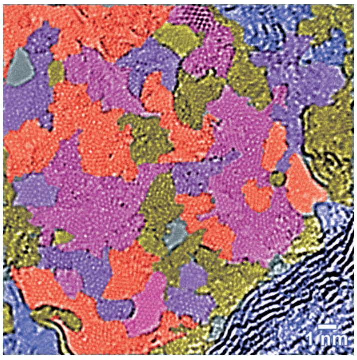

Protein Synthesis

A. O. Ogunkoya, V. R. Pattabiraman,
J. W. Bode* ______ 9693 – 9697

Sequential α-Ketoacid-Hydroxylamine (KAHA) Ligations: Synthesis of C-Terminal Variants of the Modifier Protein UFM1

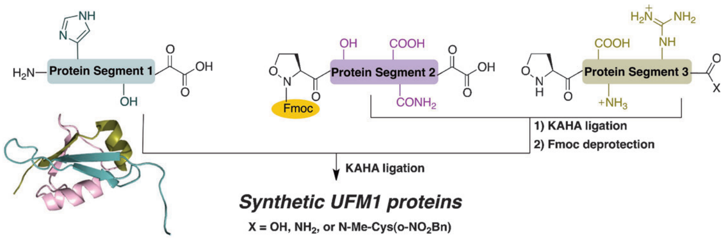

3 for 3: Sequential α-ketoacid–hydroxylamine (KAHA) ligations with 5-oxaproline allow access to the modifier protein UFM1 (Ubiquitin-fold modifier 1) with a C-terminal amide, carboxylic acid, or a masked thioester. Fmoc protection of an N-terminal 5-oxaproline permits the assembly of proteins of > 80 residues in good yield by a two-pot process from three readily prepared medium-sized protein segments.

Supporting information is available on www.angewandte.org (see article for access details).

A video clip is available as Supporting Information on www.angewandte.org (see article for access details).

This article is available online free of charge (Open Access).

This article is accompanied by a cover picture (front or back cover, and inside or outside).